

Interface structure and bias dependence of Fe/MgO/Fe tunnel junctions: *Ab initio* calculations

Christian Heiliger,* Peter Zahn,† Bogdan Yu. Yavorsky, and Ingrid Mertig
Fachbereich Physik, Martin-Luther-Universität Halle-Wittenberg, D-06099 Halle, Germany
 (Received 20 February 2006; published 27 June 2006)

Ab initio calculations of the current voltage (IV) characteristics in planar Fe/MgO/Fe tunnel junctions are presented. The electronic and magnetic structure of the junctions is calculated self-consistently in the framework of density functional theory. The bias dependence of the tunneling current and of the differential conductance is calculated in the limit of coherent tunneling for parallel and antiparallel alignment of the electrode magnetizations. Completely different IV characteristics are obtained as a function of the interface atomic structure. In agreement with experiments the tunneling magnetoresistance ratio of the tunneling current for parallel and antiparallel alignment can even change the sign as a function of bias. Details of the bias dependence are discussed in relation to the electronic structure. The obtained features of the IV characteristic can be explained by the density of states at the interfaces taking into consideration the symmetry of tunneling states.

DOI: [10.1103/PhysRevB.73.214441](https://doi.org/10.1103/PhysRevB.73.214441)

PACS number(s): 73.63.-b, 75.70.Cn, 75.30.Et, 71.15.Mb

I. INTRODUCTION

The discovery of giant magnetoresistance (GMR) was immediately accompanied by a theoretical explanation of the effect.^{1,2} Experimental results could be explained quantitatively by *ab initio* calculations.^{3,4} The revival of tunneling magnetoresistance (TMR),^{5,6} however, was characterized by a discrepancy of several orders of magnitude between experimentally and theoretically obtained values of the TMR ratio.

The origin of the discrepancy is related to the junction quality, especially the crystallinity and homogeneity of the barrier, and to the crucial role of the interface structure for the tunneling probability. A high density of structural defects, rough interfaces, and amorphous barriers cause strong scattering and tunneling in the diffusive limit. Corresponding TMR ratios do not exceed 50% at room temperature^{7,8} and could be explained by Julliere's model in terms of the spin polarization of the leads.⁹ *Ab initio* calculations of TMR, however, have been performed for structurally ideal junctions in the limit of coherent tunneling.¹⁰⁻¹² It turned out that the results for conductance and TMR are extremely sensitive to slight structural changes. Furthermore, the phenomenon of resonance tunneling occurs for highly symmetric junctions at zero bias.^{10,13} As a consequence TMR ratios up to 1000% have been predicted. These results are in contradiction to the results expected from Julliere's model and to existing experimental values.^{14,15} Nevertheless, the results obtained by different computational schemes are in very good agreement and insight into the microscopic origin of tunneling is gained.^{10,11}

A similar situation occurred for the bias dependence of the tunneling current. Experimentally obtained bias voltage characteristics of TMR up to 1 V are similar for nearly all junctions under consideration with a general decay for increasing bias, an asymmetry concerning bias reversal, and sometimes a narrow zero bias anomaly.^{8,16} In general, the tunneling characteristic of planar junctions with insulating barriers is very smooth whereas vacuum tunneling shows clear indications of the electronic structure of the leads in the bias dependencies.¹⁷

Recent experiments based on epitaxially grown samples with barriers of high crystallinity reached a new record of

TMR ratios for Fe/MgO/Fe tunnel junctions at room temperature above 200%, (Refs. 14 and 15) which exceeded the predictions by Julliere's model by far.⁹ With high quality barriers the bias voltage characteristic shows features which could be related to the electronic structure of the system.¹⁸

The role of the interface structure and material composition for tunneling was investigated in a number of experiments.¹⁹⁻²¹ In all cases a strong change of conductance and TMR was obtained. In Ref. 22 a sign reversal of the TMR ratio caused by defect states in the barrier is predicted.

The aim of this paper is to demonstrate how the interface structure can influence the bias voltage dependencies of the current, to explain special features in terms of the local density of states and the symmetry of the states. Special emphasis will be drawn on the role of coherent transport which is not included in Julliere's model.

II. JUNCTIONS

All our calculations are focused on epitaxially grown Fe/MgO/Fe systems. For these junctions very accurate data of the interface atomic structure are available.^{14,23,24}

The effect of mixed Fe/O interfaces on the electronic structure and the conductance of Fe/MgO/Fe tunnel junctions was investigated. Three types of the crystal structure (Fig. 1) are discussed. The first one has ideal Fe/MgO interfaces without mixing. This structure is possibly very close to the junctions prepared by Yuasa *et al.*¹⁴ supported by x-ray absorption spectroscopy (XAS) measurements.²⁵ The in-plane lattice constant was fixed at the experimental value for the bulk bcc Fe, $a=2.866$ Å. In correspondence to the experimental data of Ref. 26 the Fe-Fe interlayer distance next to the interface was chosen to be 1.7 Å. The remaining Fe layers are separated as in Fe bulk (1.43 Å). The distance between the interface Fe layer and the O in the first MgO layer is fixed at 2.35 Å. The first and the second MgO layer are separated by 2.25 Å, whereas the distance between the second and third MgO layer is 2.15 Å, which is close to the bulk value of MgO.

In the second junction geometry both interfaces consist of an FeO layer. The system remains symmetric and in the fol-

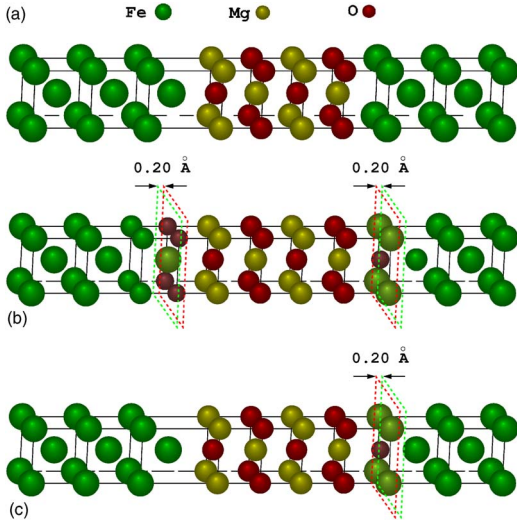


FIG. 1. (Color online) Geometric structures of the investigated junctions.

lowing text this label will be used to distinguish between the three geometries, despite that the ideal junction geometry is symmetric, too. The oxygen atoms of the FeO layer are placed close to the octahedral vacancy position shifted outward by 0.2 Å, so that the distance between these atoms and the next Mg atoms is 2.15 Å. In our study all oxygen sites were occupied, and the in-plane periodicity was kept. Partial occupancy of the FeO layer by the oxygen atoms²⁶ is not discussed in this work. The third crystal structure under consideration contains both the ideal and the FeO interface and is, of course, asymmetric. This way, we model structural differences between the left and right interface due to specific growth conditions.^{23,24,26} The interlayer distances for all three structural models correspond to the experimental data of Ref. 26 for 4.65 monolayer coverage of MgO.

III. THEORY

A. Our method

The electronic structure of the systems was calculated self-consistently within the framework of density functional theory using a screened KKR (Korringa-Kohn-Rostoker) Green's function method well suited to treat systems of dimensions comparable to experimentally investigated systems.^{27,28} The potentials were treated in the atomic sphere approximation (ASA) using local spin density approximation (LSDA) for the exchange correlation functional in the non-relativistic Schrödinger equation. For the self-consistent charge density calculations the superlattice geometry with four MgO layers sandwiched by 10 Fe layers and a cutoff for the angular momentum expansion for the Green's function of $l_{max}=3$ and for the charge density of $l_{max}=6$ was used. For the conductance calculation a system with semi-infinite Fe leads is constructed. The barrier thickness was fixed to four layers of MgO for all investigations presented.

In the ideal system the magnetic moment of the Fe interface layer was $2.83\mu_B$ similar to the Fe(001) surface. Introducing oxygen at the interface, the Fe moment is reduced to

about $2.46\mu_B$ because of the charge transfer between Fe and O. In the majority channel the Fe_{3d} states hybridize with the O_{sp} states and in the minority channel the position of the surface state close to E_F is shifted upwards by about 0.3 eV. A similar shift was confirmed in Ref. 29. The Fermi level is pinned in the central MgO layers at the top of the valence band due the angular momentum cutoff. Therefore, the potentials of the MgO layers in the middle of the barrier were shifted to adjust the Fermi level in the middle of the MgO band gap for the transport calculations.

Due to the in-plane translational invariance the eigenstates of the electrodes are labeled by the in-plane wave vector \mathbf{k}_{\parallel} . The transmission probability as introduced by Landauer³⁰ was computed using a Kubo formalism expressed in terms of the Green's function of the semi-infinite system.³¹ Our implementation in the KKR formalism including the formulation with the retarded Green's function only follows the procedure in Ref. 32 using the volume integration and an angular momentum cutoff for the derivative of $l_{max}=3$. The energy and spin dependent transmission $T^{\sigma}(E)$ is obtained by a two-dimensional integration over the surface Brillouin zone

$$T^{\sigma}(E) = \int d^2\mathbf{k}_{\parallel} T_{\mathbf{k}_{\parallel}}^{\sigma}(E), \quad (1)$$

with the transmission probability $T_{\mathbf{k}_{\parallel}}^{\sigma}(E) = \text{Tr}[J_L^{\sigma}(E)G_{LR}^{\sigma}(\mathbf{k}_{\parallel}, E)J_R^{\sigma}(E)G_{RL}^{\sigma}(\mathbf{k}_{\parallel}, E)]$. The planes L and R are situated on both sides of the barrier in the unperturbed electrode regions. $J_{L,R}^{\sigma}(E)$ are the current operator matrices and $G_{LR}^{\sigma}(\mathbf{k}_{\parallel}, E)$ are the Green's function elements connecting both sides of the junction.

Applying an external bias voltage V the chemical potentials of the electrodes μ_R and $\mu_L = \mu_R + eV$ are shifted with respect to each other which means that the potentials and the corresponding bands are shifted. Due to the small transmission we assumed a linear voltage drop inside the MgO barrier, which was confirmed by self-consistent calculations.³³ The shift of the chemical potentials was chosen symmetrical with respect to the common Fermi level $E_F = (\mu_L + \mu_R)/2$. The current density $I(V)$ is obtained by an energy integration between μ_L and μ_R to cover all tunneling states assuming $kT \ll eV$ (low temperatures) and the assumption of conduction in parallel by the two spin channels

$$I(V) = \frac{e^2}{h} \frac{1}{e} \sum_{\sigma} \int_{\mu_R}^{\mu_L} dE T(E, V),$$

$$I_{P(AP)} = I^{\uparrow\uparrow(\uparrow\uparrow)} + I^{\downarrow\downarrow(\downarrow\downarrow)}, \quad (2)$$

where $I^{\uparrow\uparrow(\uparrow\uparrow)}$ is the current from the majority spin on the left side of the junction to the majority (minority) spin on the right side for parallel (antiparallel) alignment of the electrode magnetizations. $I^{\downarrow\downarrow(\downarrow\downarrow)}$ denotes the other spin channel carried by the minority electrons of the left lead. Convergence with respect to the \mathbf{k}_{\parallel} and energy integration was better than 2%.

The current was calculated for parallel (P) and antiparallel (AP) alignment of the magnetic moments in the Fe electrodes. Due to the weak magnetic interaction between the

electrodes a frozen potential approximation was applied to construct the effective potential for the AP configuration from the P configuration without a self-consistent cycle.^{34,35}

To interpret the results the spin polarization P_I of the current is defined as follows:

$$P_I^{P(AP)} = \frac{I^{\uparrow\uparrow(\uparrow\downarrow)} - I^{\downarrow\downarrow(\downarrow\uparrow)}}{I^{\uparrow\uparrow(\uparrow\downarrow)} + I^{\downarrow\downarrow(\downarrow\uparrow)}}. \quad (3)$$

To illustrate important features of the bias characteristics the differential conductance $\frac{dI}{dV}$ is introduced. Convolution with a Gauss function of 25 meV full width at half maximum corresponding to room temperature broadening was applied to the differential conductance curves to get rid of artificial numerical peaks.

B. Comparison with Julliere's model

As we already pointed out the Julliere model is widely used to interpret experimental results in terms of the spin polarization of the leads. The idea of the following section is to estimate the deviations of the tunneling currents calculated by means of Julliere's model and in the coherent limit of tunneling. For this reason the basic formulas of the Julliere model are recalled

$$\begin{aligned} \hat{I}_P &= \hat{I}^{\uparrow\uparrow} + \hat{I}^{\downarrow\downarrow} \propto a_L a_R + (1 - a_L)(1 - a_R), \\ \hat{I}_{AP} &= \hat{I}^{\uparrow\downarrow} + \hat{I}^{\downarrow\uparrow} \propto a_L(1 - a_R) + (1 - a_L)a_R. \end{aligned} \quad (4)$$

The hat on I emphasizes that this current is estimated directly within the Julliere model. The current is proportional to the effective polarizations $a_{L,R}$ in the left and the right lead defined by

$$\begin{aligned} a_R &= \frac{n_R^\uparrow}{n_R^\uparrow + n_R^\downarrow}, \quad \text{and} \\ a_L &= \frac{n_L^\uparrow}{n_L^\uparrow + n_L^\downarrow}. \end{aligned} \quad (5)$$

Only those states are considered in the effective density of states $n_{L(R)}^{\uparrow(\downarrow)}$ for the majority (minority) spin of the left (right) lead which contribute to the current. This is a weak point of the model, since it is not defined which density of states has to be chosen.

One important conclusion of the model following Eq. (4) is that

$$\hat{I}^{\uparrow\uparrow}\hat{I}^{\downarrow\downarrow} = \hat{I}^{\uparrow\downarrow}\hat{I}^{\downarrow\uparrow}. \quad (6)$$

This relation holds also with an external bias, since the bias dependence of the current is incorporated in the Julliere model via effective polarizations $a_L(V)$ and $a_R(V)$ at a certain bias voltage V .²¹

The deviations from the identity in Eq. (6) are a measure to assess the influence of the transmission coefficients neglected in the Julliere model. The larger the deviations of the spin dependent currents from Eq. (6) the more important is the influence of the transmission coefficients and an explicit

treatment of them is necessary. Even if Eq. (6) is fulfilled it is still unclear which states contribute to the effective polarizations $a_L(V)$ and $a_R(V)$.

Now the question should be answered how large the error in the Julliere model is if Eq. (6) is violated. To estimate the deviation a proportionality constant $f(V)$ is defined

$$I_P(V) \propto f(V)[a_L(V)a_R(V) + (1 - a_L(V))(1 - a_R(V))]$$

$$I_{AP}(V) \propto a_L(V)(1 - a_R(V)) + (1 - a_L(V))a_R(V). \quad (7)$$

These currents cannot be directly estimated within the Julliere model if $f(V) \neq 1$. Therefore, these quantities have no hat to make them distinct from the currents of Eq. (4). All quantities depend explicitly on bias voltage V . Consequently Eq. (6) is transformed into

$$I^{\uparrow\uparrow}(V)I^{\downarrow\downarrow}(V) = f^2(V)I^{\uparrow\downarrow}(V)I^{\downarrow\uparrow}(V). \quad (8)$$

The quantity $f(V)$ can be derived via Eq. (8) from our bias characteristics calculated in the limit of coherent transport. The deviations of $f(V)$ from unity indicate that the averaged transmission probabilities are different for the P and AP configuration. In contradiction, in the Julliere model all contributing states have the same transmission probability independent of the magnetic order.

Based on the current densities estimated by Eq. (4) and calculated by means of Eq. (7) the corresponding TMR ratios are derived

$$\begin{aligned} \left(\frac{\Delta I}{I}\right)_{jul} &= \frac{\hat{I}_P(V) - \hat{I}_{AP}(V)}{\hat{I}_{AP}(V)}, \\ \frac{\Delta I}{I} &= \frac{I_P(V) - I_{AP}(V)}{I_{AP}(V)}. \end{aligned} \quad (9)$$

The definition of the TMR ratio used here differs from that used in a previous publication.³⁶ The current densities $I_P(V)$ and $I_{AP}(V)$ are the main ingredients for both equations. This definition was chosen to allow for a simple comparison with the results applying Julliere's model in terms of the quantity $f(V)$. $\left(\frac{\Delta I}{I}\right)_{jul}$ describes the TMR ratio obtained from our IV characteristics mapping the currents to effective polarizations by Eq. (4) and (6). Using Eqs. (9) and (7) one obtains

$$\left(\frac{\Delta I}{I}\right)_{jul} = \frac{1}{f(V)} \left(\frac{\Delta I}{I} - f(V) + 1 \right). \quad (10)$$

In the discussion of our results this equation is used to estimate the difference on the level of TMR between the Julliere model and a coherent treatment of the transport.

IV. RESULTS

A. Current voltage characteristics

The calculated bias dependence of the current density $I(V)$, of the spin polarization $P_I(V)$ of the current and of the differential conductance are shown in Fig. 2 for all considered junctions and both magnetic configurations. The spin contributions to the differential conductance for P (AP)

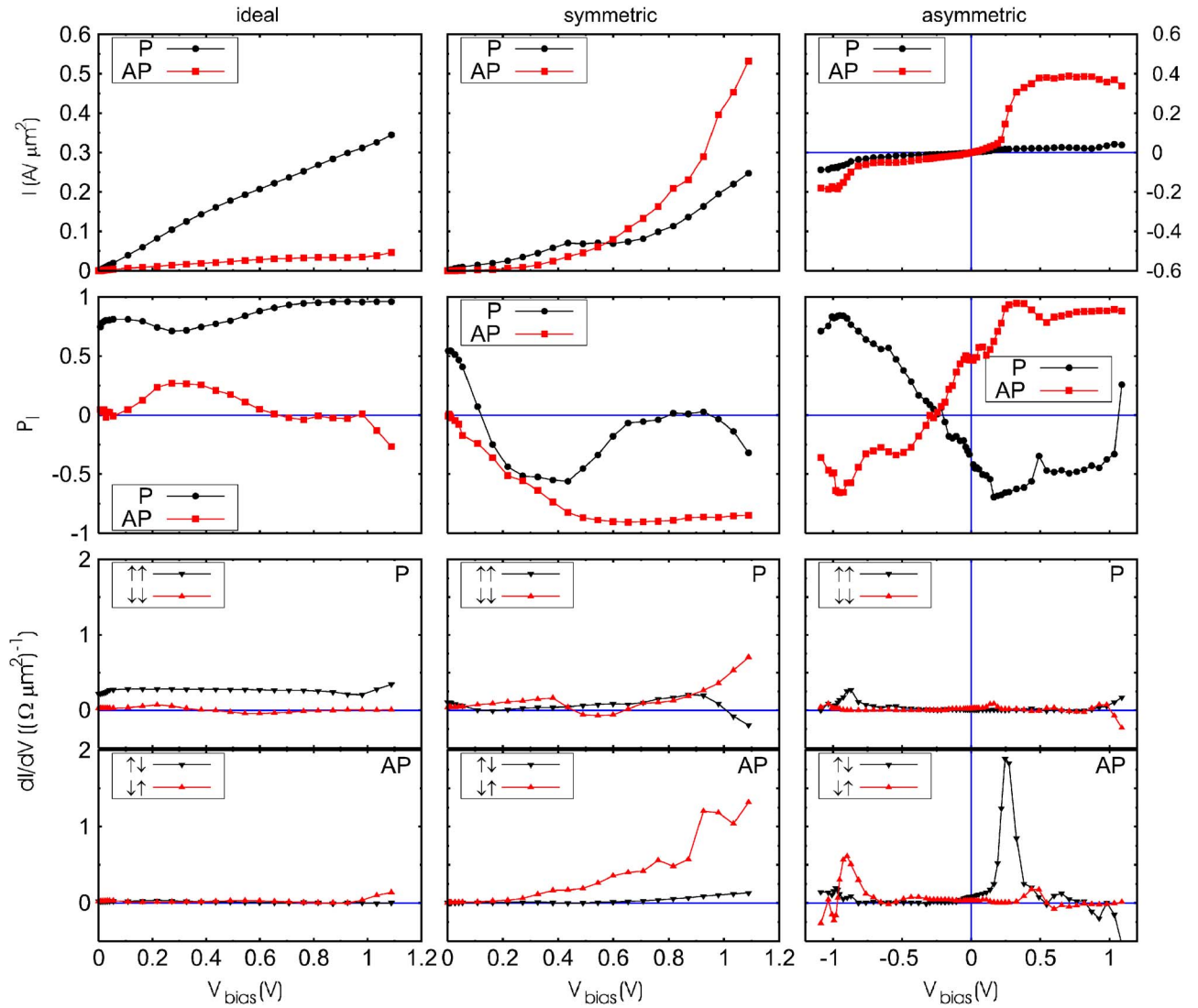


FIG. 2. (Color online) Bias dependence of the current I , the polarization of the current P_I , and of the differential conductance $\frac{dI}{dV}$ for all considered junction geometries; left: ideal; middle: symmetric; right: asymmetric (see Fig. 1).

alignment are labeled $\uparrow\uparrow(\uparrow\downarrow)$ and $\downarrow\downarrow(\downarrow\uparrow)$ for minority and majority spin in the left electrode, respectively. For the ideal junction we obtain a nearly linear current dependence in both magnetic configurations. This behavior is reflected in a nearly constant differential conductance. The polarization changes slightly. For the P configuration the current is highly polarized larger than 80%, which means that almost only the majority spin channel contributes to the transport. For higher voltages this aspect is even more pronounced. In the AP configuration the current is almost unpolarized.

A similar behavior of the current was found for all junctions in the P configuration. This means, that the current is linearly dependent on the external bias in contrast to the current in the AP configuration of the symmetric and asymmetric junction. In the P configuration the polarization shows strong changes as a function of the voltage.

An important feature of the symmetric junction is, that the current in the AP alignment is strongly increasing with increasing bias. Almost the whole current is carried by the minority spin channel. The current in the minority spin chan-

nel increases strongly with bias, which is reflected in the differential conductance. This behavior leads to a higher current density in the AP than in the P configuration for voltages larger than 0.57 V. For this reason the TMR ratio changes the sign at this bias as was already reported.³⁶

In the asymmetric junction the current in the AP configuration is higher than for P alignment at all bias voltages, which causes a negative TMR ratio over the whole voltage range. The polarization of the current is generally very high at high voltages, but the dominating spin channel changes at about -0.2 V for both magnetic configurations. A striking feature is the resonance in the differential conductance of the AP configuration at about 0.33 V, which is related to the strong increase of the current. This resonance is essential to explain³⁶ the results of bias dependent measurements of the TMR ratio in Fe/MgO/Fe tunnel junctions.²⁹ There are additional features like the resonances at -0.95 V in both magnetic configuration.

The main objective of the following analysis is to understand the origin of these features. For this reason the origin

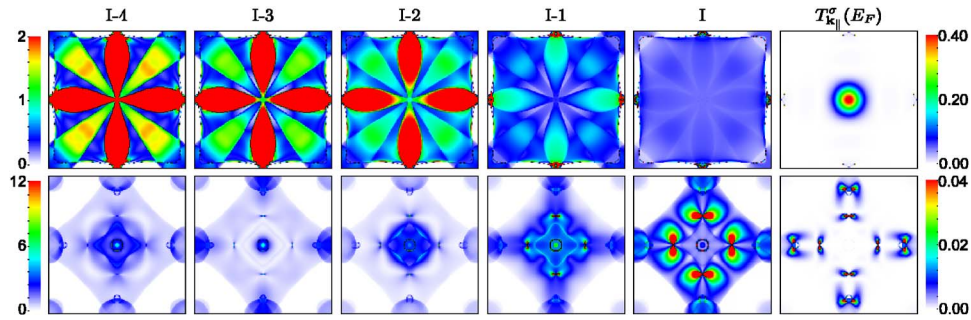


FIG. 3. (Color online) \mathbf{k}_{\parallel} -resolved LDOS of the ideal junction are shown in the surface Brillouin zone, starting from left the 5th Fe layer from the interface (I-4) up to the Fe layer at the interface (I). The right column shows the corresponding transmissions $T_{\mathbf{k}_{\parallel}}^{\sigma}(E_F)$ for zero bias. Top row: majority spin; bottom row: minority spin.

of the resonance in the differential conductance at 0.33 V will be discussed in detail. In particular, the first step is to analyze the density of states and their relation to the conductance.

B. Local DOS versus zero bias conductance

The main question is if the conductance can be related to the local density of states (LDOS). For this reason the \mathbf{k}_{\parallel} -resolved LDOS at E_F for the ideal structure for different layers and the corresponding \mathbf{k}_{\parallel} -resolved transmission coefficients for zero bias are compared in Fig. 3. It is obvious that only the LDOS at the Fe interface layers has features in common with the transmission. In the minority spin channel the symmetry of the transmission is only reflected in the LDOS at the interface layer. The pronounced d -like states in the majority spin channel visible in the LDOS far away from the interface layer are not reflected in the transmission. The LDOS of the interface layer is much smaller than in the bulk region (compare layer I and I-4) and is dominated by more delocalized states of sp -character. The current in the majority spin channel is dominated by states with Δ_1 symmetry, which explains the central peak of conductance in the center of the Brillouin zone caused by the rapidly decreasing transmission probability with an increasing angle of incidence.

On the other hand, the DOS is not the only part that determines the transport coefficients. The other important ingredient is the matrix element which acts like a filter and determines to which amount a particular state in the \mathbf{k}_{\parallel} -space contributes to the current. These matrix elements are included by the evaluation of Eq. (1) using the Green's function of the whole junction. Our calculational scheme determines the current contributions from all states in the Brillouin zone, which differ by orders of magnitude. These differences cannot be described by the Julliere model, since they require the quantum mechanical description of the whole tunneling process.

In conclusion, the LDOS together with the corresponding matrix elements determine the transport coefficients. The importance of the matrix elements is confirmed by the IV characteristics presented in Fig. 2, since the only difference between the investigated geometries is the structure of the interface layers.

C. Transmission resonances

As already pointed out, our aim is to understand the origin of the resonance in the differential conductance of the asym-

metric junction in the AP configuration. The importance of the LDOS at the interface was already emphasized. For this reason the spin-dependent LDOS of Fe at the left and right interface layer shifted according to a bias voltage of 0.33 V are shown in Fig. 4. With the help of the polarization (see Fig. 2, right column middle panel) we know that the current is carried almost by the majority electrons of the left lead. Therefore, only the majority electrons of the left lead and the minority electrons of the right lead have to be considered. The interval for the energy integration between μ_R and μ_L is marked in Fig. 4. At the FeO interface layer there is a peak in the DOS of the minority spin, which was also observed by other groups.²⁹ They claimed that this peak is the reason for an experimentally observed strong increase of the current at a particular bias voltage. From our analysis it is evident that even when the maximum of the peak is not yet inside the energy integration interval [see Eq. (2)], a resonance in the current occurs.

To analyze this behavior the transmission $T(E, V)$ is shown for various applied voltages in Fig. 5. The integration

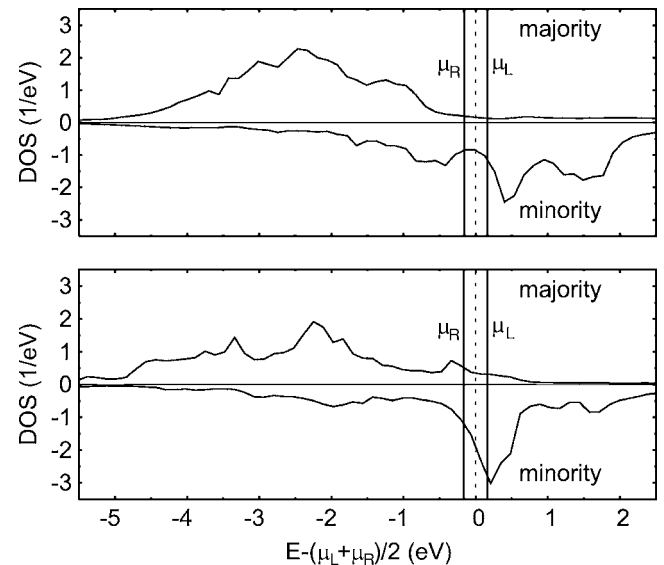


FIG. 4. The LDOS of Fe in the interface layer of the asymmetric junction at a voltage of about 0.33 V. Top: at the left interface without oxygen; bottom: at the right interface with oxygen; The integration window corresponding to the applied voltage is marked by the vertical lines.

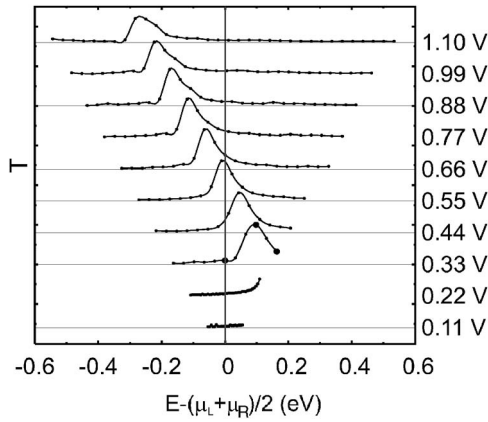


FIG. 5. Transmission $T^{\uparrow\downarrow}(E)$ for different bias voltages of the asymmetric junction in the AP configuration.

over these curves leads to the corresponding currents $I(V)$ [see Eq. (2)]. For a voltage of about 0.22 V a peak appears at the upper bound of the integration interval and shifts for larger voltages to lower energies, which means that the peak is closely linked to certain states at the right interface. To classify this resonance the spin-dependent \mathbf{k}_{\parallel} -resolved LDOS and the transmission $T(E)$ are compared for certain energies in the integration interval for a bias voltage of 0.33 V in Fig. 6. The three chosen energy values are marked on the $T(E)$ curve in Fig. 5 by dots. In the AP magnetic configuration the majority spin channel has majority character in the left electrode and minority character in the right electrode. For this reason the \mathbf{k}_{\parallel} -resolved LDOS of majority spin in the left Fe

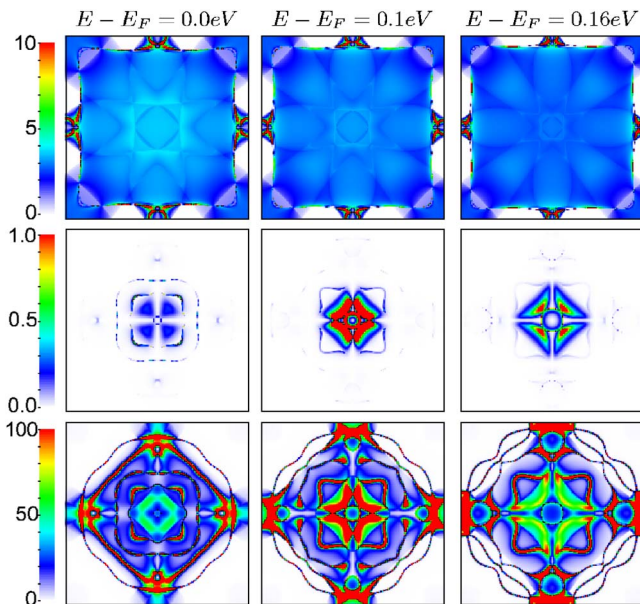


FIG. 6. (Color online) Asymmetric junction in AP configuration: \mathbf{k}_{\parallel} -resolved LDOS and transmission $T_{\mathbf{k}_{\parallel}}^{\uparrow\downarrow}(E)$ at bias $V=0.33$ V. left column $E-E_F=0.0$ eV, middle $E-E_F=0.1$ eV, right $E-E_F=0.16$ eV (marked in Fig. 6), top row: majority LDOS of left Fe interface layer (without oxygen), bottom row: minority LDOS of right Fe interface layer (with mixed FeO layer), middle row: transmission $T_{\mathbf{k}_{\parallel}}^{\uparrow\downarrow}(E)$.

interface layer and of minority spin in the right interface layer are compared with the \mathbf{k}_{\parallel} -resolved transmission. The reason for the peak at about $E-E_F=0.10$ eV in the transmission $T(E)$ becomes obvious. At this energy electronic states of local minority character exist in the right electrode close to the center of the Brillouin zone, which show a large probability amplitude in the Fe interface layer. Because of the *sp*-like character of the states in the left electrode (see LDOS in Fig. 6, the upper row), which are available for many \mathbf{k}_{\parallel} vectors, electrons from these states can most easily tunnel through the barrier into the right lead. At higher energies the LDOS in the Brillouin zone center attenuates again and very few final states in the right electrode are available. This causes the transmission to level off for energies higher than the resonance. Since the interface resonance is a local property of the mixed FeO interface its position shifts according to the applied external bias voltage to lower energies. These states are only a small contribution to the total LDOS in this atomic layer. For this reason the \mathbf{k}_{\parallel} -integrated LDOS shown in Fig. 4 cannot give a clue for a high transmission, because only a small number of states carries the dominant part of the current.

The peculiarity is also very pronounced in the symmetric junction. This junction has identical interfaces with mixed FeO layers. The LDOS is the same as shown in Fig. 4, bottom panel, with a peak above the Fermi level for the minority spin channel. The IV characteristic for the AP configuration of the symmetric junction, however, does not show the same peculiarities as the asymmetric junction. The reason for the absence is given by the tunneling matrix elements, which reflect the fact that the electronic states at both interfaces do not match. The different shape of majority DOS close to E_F at the interface without oxygen (Fig. 4, top panel) and with a mixed FeO layer (Fig. 4, bottom panel) points to the different character of the states available for tunneling. This comparison shows that the evaluation of matrix elements is essential to understand the formation of the tunneling current and its behavior with an applied external bias voltage.

D. Comparison to Julliere's model

To emphasize the importance of a description in the coherent limit of the transport through a crystalline barrier the deviations using the simple idea of the Julliere model are visualized explicitly. It was already pointed out in Sec. III B that within the Julliere model the different transmission probabilities of the contributing states in the P and AP magnetic configurations are neglected. In Eq. (7) the quantity $f(V)$ was introduced to measure the difference in the averaged transmission probability of P and AP magnetic configuration derived from the spin-dependent currents. Furthermore, from the spin-dependent currents comprised in the IV characteristics in Fig. 2 the quantity $f(V)$ is calculated for all junction geometries using Eq. (8) and is shown in Fig. 7.

In the Julliere model $f(V)$ is assumed to be one. The calculations in the coherent limit, however, show large deviations of $f(V)$ for all types of junctions. As a measure of the deviation the relative difference of the TMR ratio $\Delta I/I$ derived from the IV characteristics and the TMR ratio $(\Delta I/I)_{jul}$

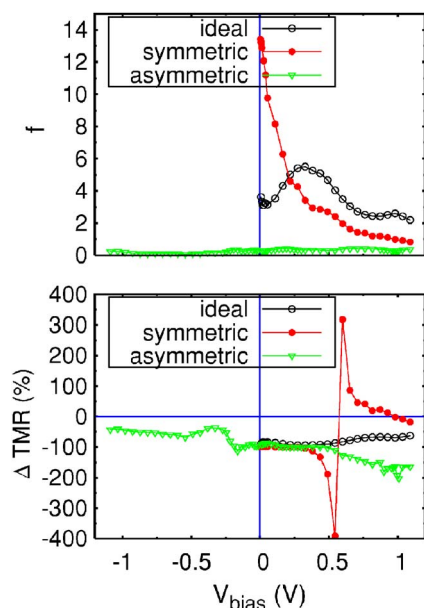


FIG. 7. (Color online) The proportionality constant referring to Eq. (8) and the relative error of the TMR using the Julliere model are shown.

including the restrictions by the Julliere model $\Delta TMR = \frac{\Delta I/I - (\Delta I/I)_{Jull}}{\Delta I/I}$ is introduced and discussed in the bottom panel of Fig. 7. The deviations are very large for all junction ge-

ometries and reveal the shortcomings of the Julliere model assuming a constant transmission probability for both magnetic configurations.

V. CONCLUSION

In conclusion, the tunneling conductance of single crystalline Fe/MgO/Fe tunnel junctions was calculated for different interface geometries as a function of the applied bias voltage without adjustable parameters except the assumed potential profile under the influence of an applied bias voltage. The modification of the interfaces allows the generation of completely different bias voltage dependencies. Special features of the bias characteristics such as resonances are determined by the interface geometry and the related electronic structure. In particular, the local density of states at the interface layers and the symmetry of the eigenstates in the leads are of special importance. In addition, we have shown that the properties of the IV characteristics and the TMR ratio dependence on external bias voltage are not reproducible within a Julliere model.

ACKNOWLEDGMENTS

We thank P. M. Levy, P. Bruno, J. Henk, and A. Ernst for fruitful discussions. Financial support by the DFG (FG 404) is kindly acknowledged.

*Electronic address: christian.heiliger@physik.uni-halle.de

†Electronic address: peter.zahn@physik.uni-halle.de

- ¹M. N. Baibich, J. M. Broto, A. Fert, F. N. V. Dau, F. Petroff, P. Etienne, G. Creuzet, A. Friederich, and J. Chazelas, *Phys. Rev. Lett.* **61**, 2472 (1988).
- ²G. Binasch, P. Grünberg, F. Saurenbach, and W. Zinn, *Phys. Rev. B* **39**, 4828 (1989).
- ³K. M. Schep, P. J. Kelly, and G. E. W. Bauer, *Phys. Rev. Lett.* **74**, 586 (1995).
- ⁴P. Zahn, I. Mertig, M. Richter, and H. Eschrig, *Phys. Rev. Lett.* **75**, 2996 (1995).
- ⁵J. S. Moodera, L. R. Kinder, T. M. Wong, and R. Meservey, *Phys. Rev. Lett.* **74**, 3273 (1995).
- ⁶T. Miyazaki and N. Tezuka, *J. Magn. Magn. Mater.* **139**, L231 (1995).
- ⁷S. Parkin, K. Roche, M. Samant, P. Rice, R. Beyers, R. Scheuerlein, E. O'Sullivan, S. Brown, J. Bucchigano, D. Abraham *et al.*, *J. Appl. Phys.* **85**, 5828 (1999).
- ⁸X.-F. Han, T. Daibou, M. Kamijo, K. Yaoita, H. Kubota, Y. Ando, and T. Miyazaki, *Jpn. J. Appl. Phys., Part 2* **39**, L439 (2000).
- ⁹M. Julliere, *Phys. Rev. Lett.* **54A**, 225 (1975).
- ¹⁰W. H. Butler, X.-G. Zhang, T. C. Schulthess, and J. M. MacLaren, *Phys. Rev. B* **63**, 054416 (2001).
- ¹¹J. Mathon and A. Umerski, *Phys. Rev. B* **63**, 220403(R) (2001).
- ¹²D. Wortmann, G. Bihlmayer, and S. Blügel, *J. Phys.: Condens. Matter* **16**, 5819 (2004).
- ¹³O. Wunnicke, N. Papanikolaou, R. Zeller, P. H. Dederichs, V.

- Drchal, and J. Kudrnovský, *Phys. Rev. B* **65**, 064425 (2002).
- ¹⁴S. Yuasa, T. Nagahama, A. Fukushima, Y. Suzuki, and K. Ando, *Nat. Mater.* **3**, 868 (2004).
- ¹⁵S. Parkin, C. Kaiser, A. Panchula, P. Rice, B. Hughes, M. Samant, and S.-H. Yang, *Nat. Mater.* **3**, 862 (2004).
- ¹⁶S. Yuasa, T. Sato, E. Tamura, Y. Suzuki, H. Yamamori, K. Ando, and T. Katayama, *Europhys. Lett.* **52**, 344 (2001).
- ¹⁷H. F. Ding, W. Wulfhekel, J. Henk, P. Bruno, and J. Kirschner, *Phys. Rev. Lett.* **90**, 116603 (2003).
- ¹⁸J. Faure-Vincent, C. Tiusan, E. Jouguelet, F. Canet, M. Sajjeddine, C. Bellouard, E. Popova, M. Hehn, F. Montaigne, and A. Schuhl, *Appl. Phys. Lett.* **82**, 4507 (2003).
- ¹⁹P. LeClair, H. J. M. Swagten, J. T. Kohlhepp, R. J. M. van de Veerdonk, and W. J. M. de Jonge, *Phys. Rev. Lett.* **84**, 2933 (2000).
- ²⁰P. LeClair, J. T. Kohlhepp, H. J. M. Swagten, and W. J. M. de Jonge, *Phys. Rev. Lett.* **86**, 1066 (2001).
- ²¹J. M. De Teresa, A. Barthélémy, A. Fert, J. P. Contour, R. Lyonnet, F. Montaigne, P. Seneor, and A. Vaurès, *Phys. Rev. Lett.* **82**, 4288 (1999).
- ²²E. Y. Tsymlal, A. Sokolov, I. F. Sabirianov, and B. Doudin, *Phys. Rev. Lett.* **90**, 186602 (2003).
- ²³H. L. Meyerheim, R. Popescu, J. Kirschner, N. Jedrecy, M. Sauvage-Simkin, B. Heinrich, and R. Pinchaux, *Phys. Rev. Lett.* **87**, 076102 (2001).
- ²⁴C. Tusche, H. L. Meyerheim, N. Jedrecy, G. Renaud, A. Ernst, J. Henk, P. Bruno, and J. Kirschner, *Phys. Rev. Lett.* **95**, 176101

- (2005).
- ²⁵K. Miyokawa, S. Saito, T. Katayama, T. Saito, T. Kamino, K. Hanashima, Y. Suzuki, K. Mamiya, T. Koide, and S. Yuasa, *Jpn. J. Appl. Phys., Part 2* **44**, L9 (2005).
- ²⁶H. L. Meyerheim, R. Popescu, N. Jedrecy, M. Vedpathak, M. Sauvage-Simkin, R. Pinchaux, B. Heinrich, and J. Kirschner, *Phys. Rev. B* **65**, 144433 (2002).
- ²⁷R. Zeller, P. H. Dederichs, B. Újfalussy, L. Szunyogh, and P. Weinberger, *Phys. Rev. B* **52**, 8807 (1995).
- ²⁸N. Papanikolaou, R. Zeller, and P. Dederichs, *J. Phys.: Condens. Matter* **14**, 2799 (2002).
- ²⁹C. Tiusan, J. Faure-Vincent, C. Bellouard, M. Hehn, E. Jouguelet, and A. Schuhl, *Phys. Rev. Lett.* **93**, 106602 (2004).
- ³⁰R. Landauer, *Z. Phys. B* **68**, 217 (1987).
- ³¹H. U. Baranger and A. D. Stone, *Phys. Rev. B* **40**, 8169 (1989).
- ³²P. Mavropoulos, N. Papanikolaou, and P. H. Dederichs, *Phys. Rev. B* **69**, 125104 (2004).
- ³³C. Zhang, X.-G. Zhang, P. S. Krstić, H. P. Cheng, W. H. Butler, and J. M. MacLaren, *Phys. Rev. B* **69**, 134406 (2004).
- ³⁴D. Pettifor, *Commun. Phys. (London)* **1**, 141 (1976).
- ³⁵D. Pettifor and C. Varma, *J. Phys. C* **12**, L 253 (1979).
- ³⁶C. Heiliger, P. Zahn, B. Y. Yavorsky, and I. Mertig, *Phys. Rev. B* **72**, 180406(R) (2005).